

**Fundamental Studies to Enable Robust,  
Reliable, Low Emission Gas Turbine  
Combustion of High Hydrogen Content  
Fuels:** experimental and computational studies

**Margaret Wooldridge**

Arthur F. Thurnau Professor,  
Departments of Mechanical and Aerospace Engineering,  
University of Michigan, Ann Arbor

2011 University Turbine Systems  
Research Workshop  
November 30<sup>th</sup>, 2011  
WebEx

**Graduate student  
contributors:**

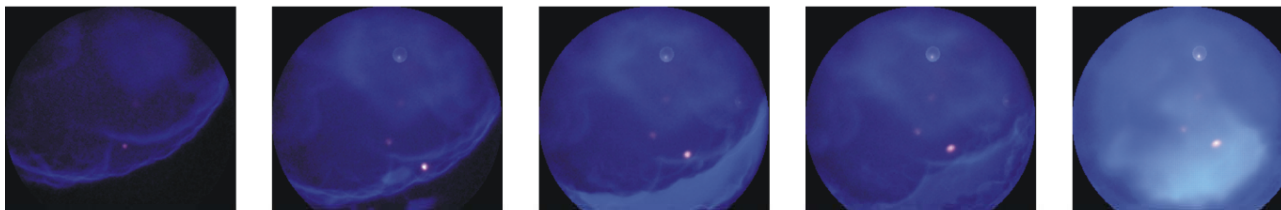
Andrew Mansfield, Stephen  
Walton

**Co-PIs:**

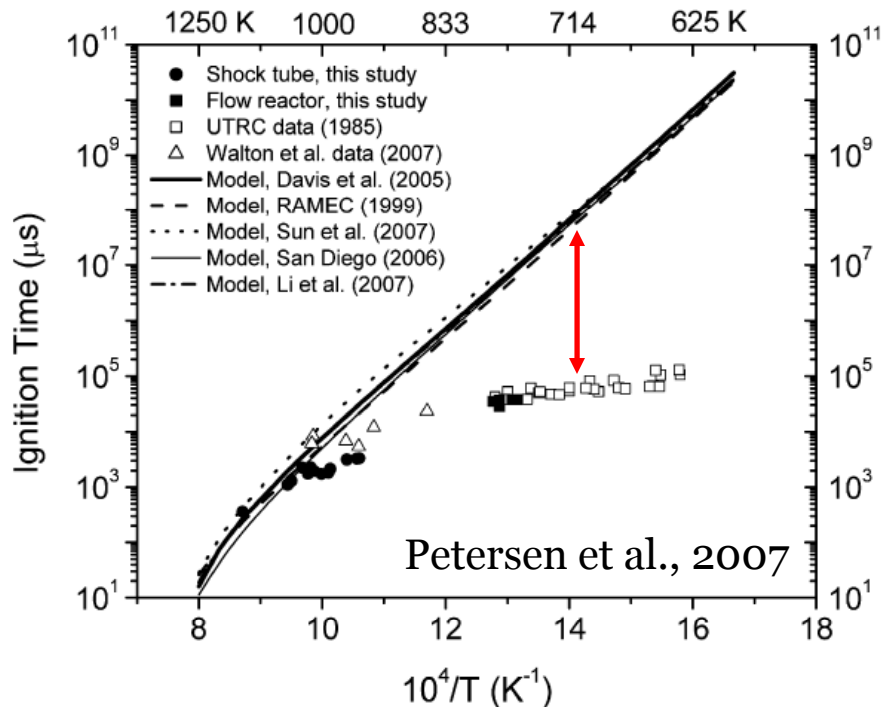
Hong Im, Professor  
Department of Mechanical  
Engineering,  
University of Michigan

Charles Westbrook, Scientist  
Lawrence Livermore National  
Laboratory

## outline



*Background and motivation*  
*Experimental results*  
*Computational plan of work*



**Discrepancy in ignition delay between the experiments and numerical modeling approaches has not been understood properly**

Possible explanations:

- Uncertainties in rate coefficients
- Incomplete reaction mechanisms
- Surface-catalytic mechanisms
- Ignition regimes
- Wall heat transfer
- Turbulence (Ihme, C&F, 2012)

- $H_2/CO$  combustion chemistry experiments are highly sensitive to mixture composition including trace impurities.
- Recent studies indicate some reactions are missing from high temperature reaction mechanisms that are important at low temperatures and high pressures.
- 3<sup>rd</sup> body collisions efficiencies may need refinement.
- Experimental data and modeling approaches are convolved with uncertainties in initial conditions, boundary conditions, and process assumptions, to name a few important considerations.
- Until recently, there were few experimental data for validating syngas combustion kinetics at gas turbine conditions. We now have a lot more experimental data to consider.

Walton et al. (2007)<sup>1</sup> evaluated syngas ignition in UM-RCF

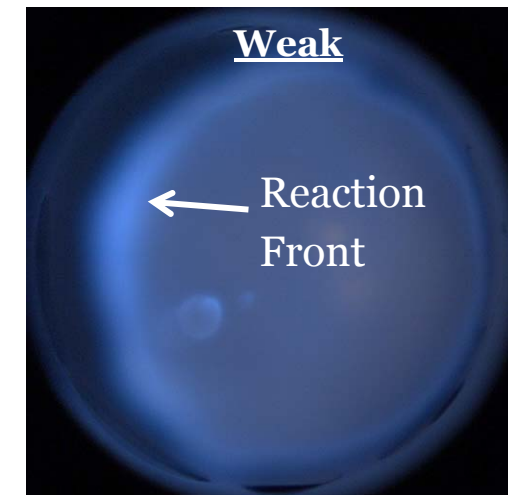
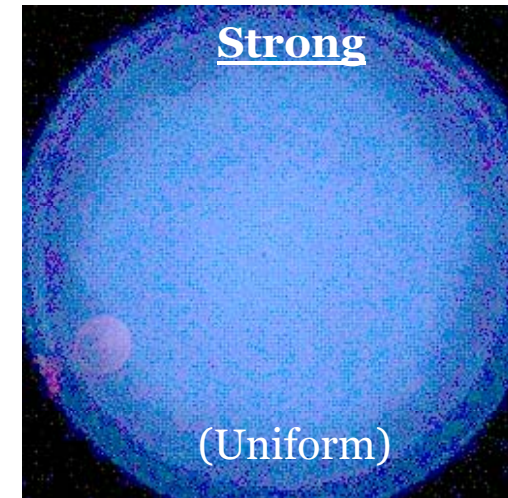
- Measured  $\tau_{\text{ignition}}$  for lean dilute low temp., high pressure, H<sub>2</sub>/CO mixtures, using pressure time histories during ignition
- Identified spatial features of ignition (weak and strong) using high speed imaging

Walton et al. (2007)<sup>2</sup> evaluated iso-octane ignition in UM-RCF

- High speed imaging also used to identify spatial features of ignition (weak and strong)
- Proposed a critical fuel mole fraction marks the transition between strong and weak ignition.
- Propagation speeds of reaction fronts  $\gg$  Laminar flame speed
- Ignition theory implied thermal gradients were responsible for observed speeds and gradients were consistent with  $\sim$ experimental values

Walton, He, Zigler, Wooldridge (2007) "An experimental investigation of the ignition properties of hydrogen and carbon monoxide mixtures for syngas turbine applications," *Proc. Combust. Inst.* **31** 3147-3154.

Walton, He, Zigler, Wooldridge, Atreya (2007) "An experimental investigation of iso-octane ignition phenomena," *Combust. Flame*, **150** 246-262.



Images during ignition of syngas in UM-RCF experiments

Top:  $T = 1028 \text{ K}$ ,  $P = 7.6 \text{ atm}$ ,  $\phi = 0.15$ .

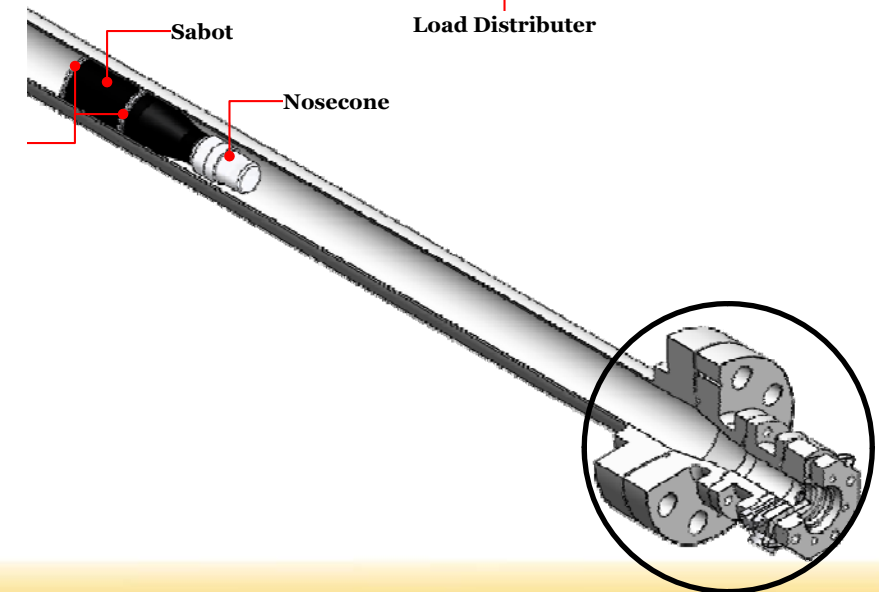
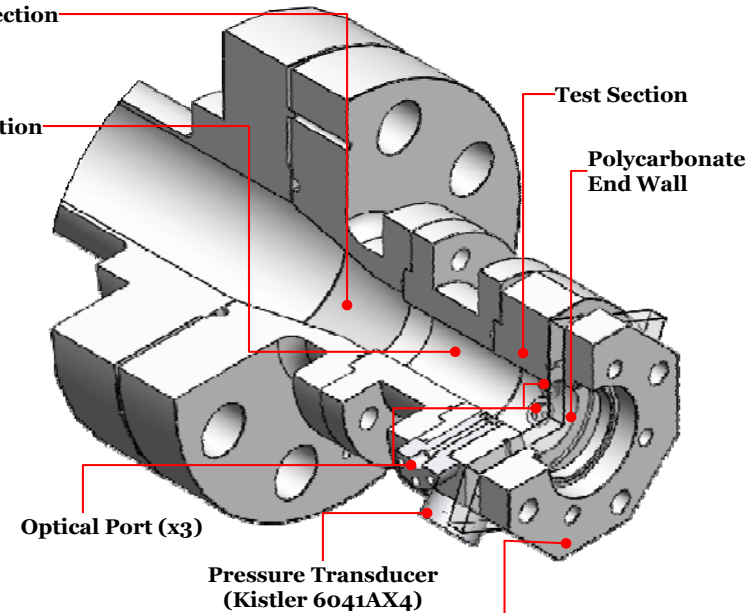
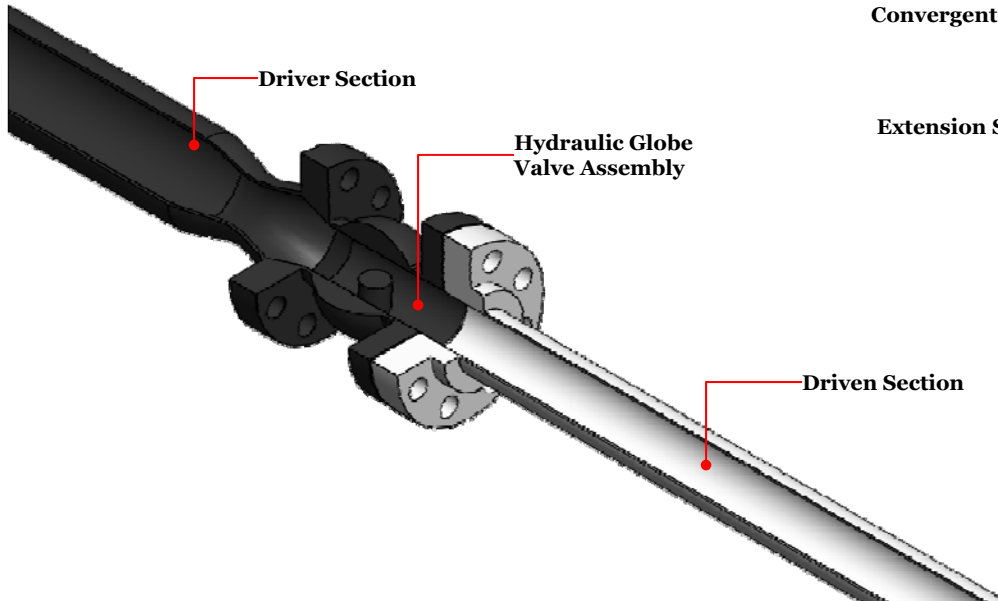
Bottom:  $T = 1006 \text{ K}$ ,  $P = 2.71 \text{ atm}$ ,  $\phi = 0.5$ .

The proposed research program focuses on three areas to advance syngas turbine design:

1. syngas chemistry
2. fundamental ignition and extinction limits of HHC fuels
3. data distillation for rapid transfer of knowledge to gas turbine design.

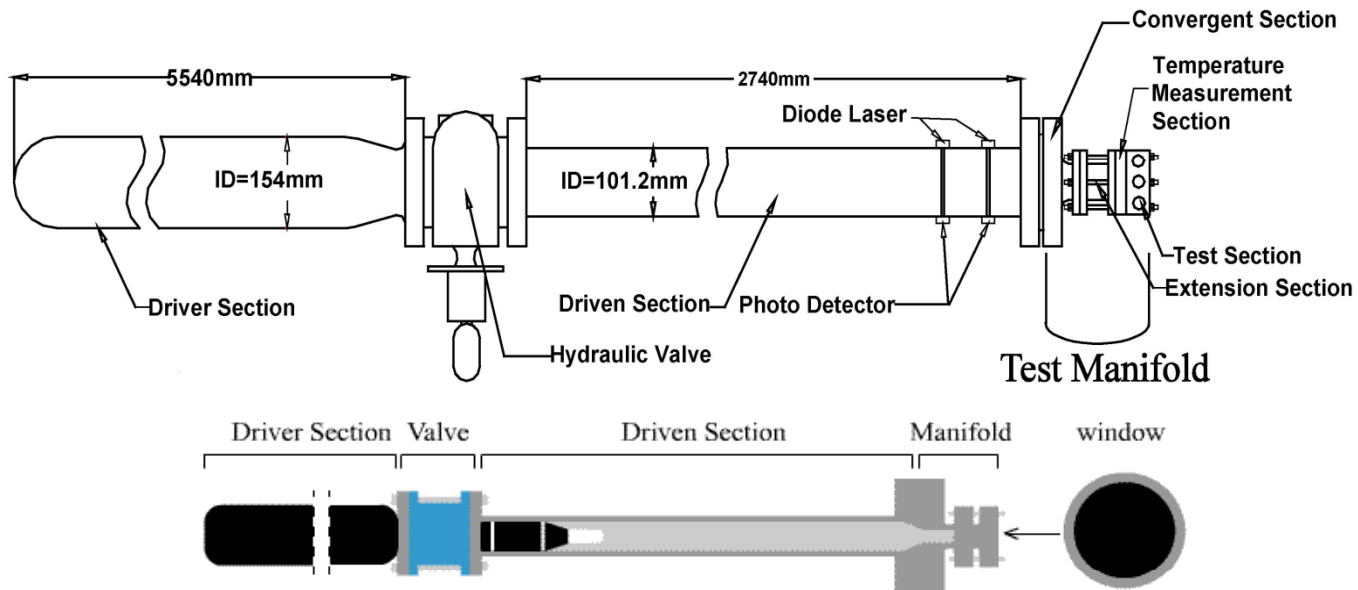
The project objectives are:

1. To develop and validate an accurate and rigorous experimental and computational data base of HHC reaction kinetics, flame speeds and flammability limits of HHC fuels including mixtures with high levels of exhaust gases,
2. To develop detailed and reduced HHC chemical mechanisms that accurately reproduce the new experimental data as well as data in the literature,
3. To develop a quantitative understanding of the stability of HHC combustion to fluctuations in the flow field, including the opportunities and challenges of exhaust gas recirculation (EGR) on extinction, ignition and flame stability,
4. To develop domain maps which identify the range of conditions (e.g. % EGR) where HHC combustion can be effected in both positive and negative manners (e.g. expanded/restricted flammability limits).

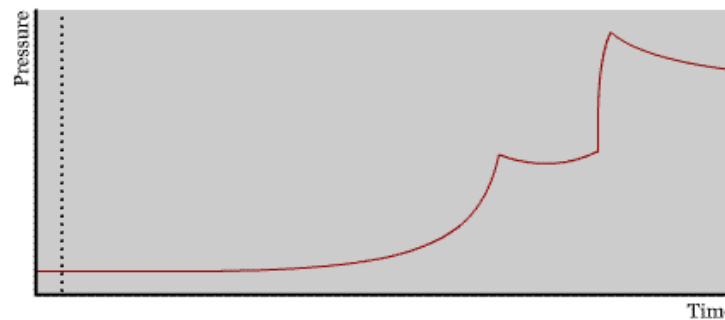


## UM RCF Dimensions:

- Driver section: 5.54 m, ID 154 mm, carbon steel
- Driven section: 2.74 m, ID 101.2 mm, chromed and honed stainless steel
- Convergent section: ID 101.6-50.8 mm
- Extension sections: 81 mm, 126 mm, ID 50.8 mm
- Thermocouple sections: 16.2 mm, 25.4 mm, ID 50.8 mm
- Large test volume  $\sim 200 \text{ cm}^3$
- Volume-to-surface area ratio of 0.8 – 1.1



$$P_{eff} = \frac{1}{\frac{t_{dp}}{\frac{dp}{dt}_{max}} - t_{P_{max}} \frac{t_{dp}}{\frac{dp}{dt}_{max}}} \int_{t_{P_{max}}}^{\frac{t_{dp}}{\frac{dp}{dt}_{max}}} P dt$$



$$\int_{T_0}^{T_{eff}} \frac{\gamma}{\gamma - 1} d \ln T = \ln \left( \frac{P_{eff}}{P_0} \right)$$

## Results: high speed imaging of weak syngas ignition

- $T = 1006 \text{ K}$ ,  $P = 2.71 \text{ atm}$
- Inert gas:  $\text{O}_2$  ratio = 5.91
- $\phi = 0.5$ ,
- 5.04%  $\text{H}_2$ , 7.26%  $\text{CO}$

Weak ignition characterized by spatially resolved ignition features followed by volumetric ignition.

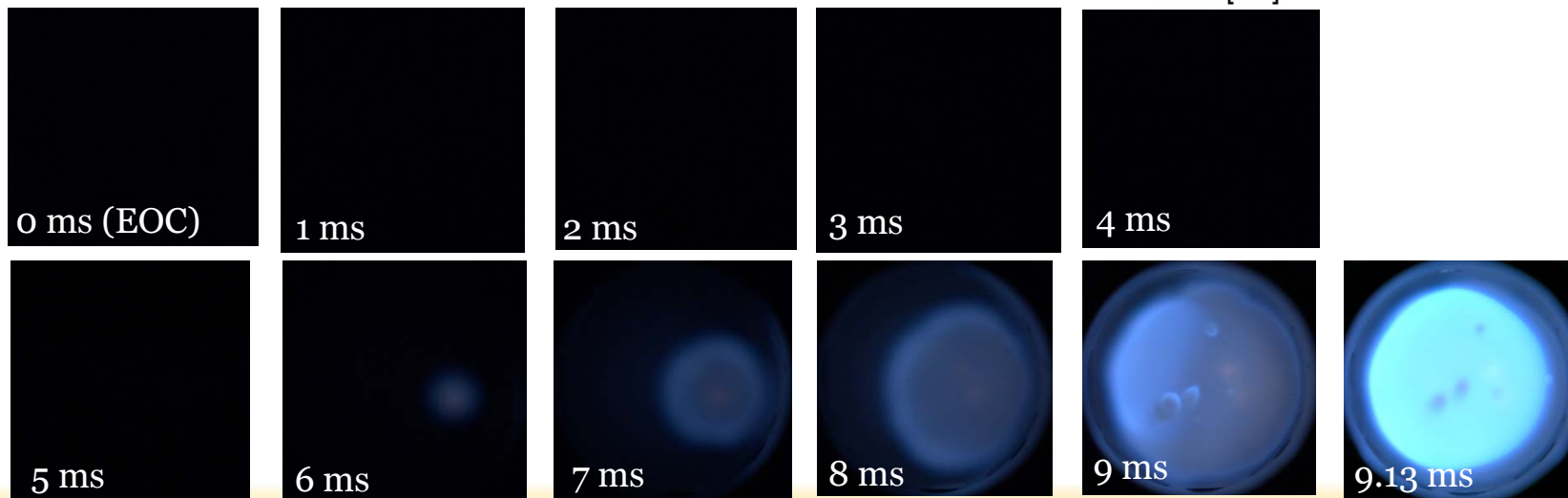
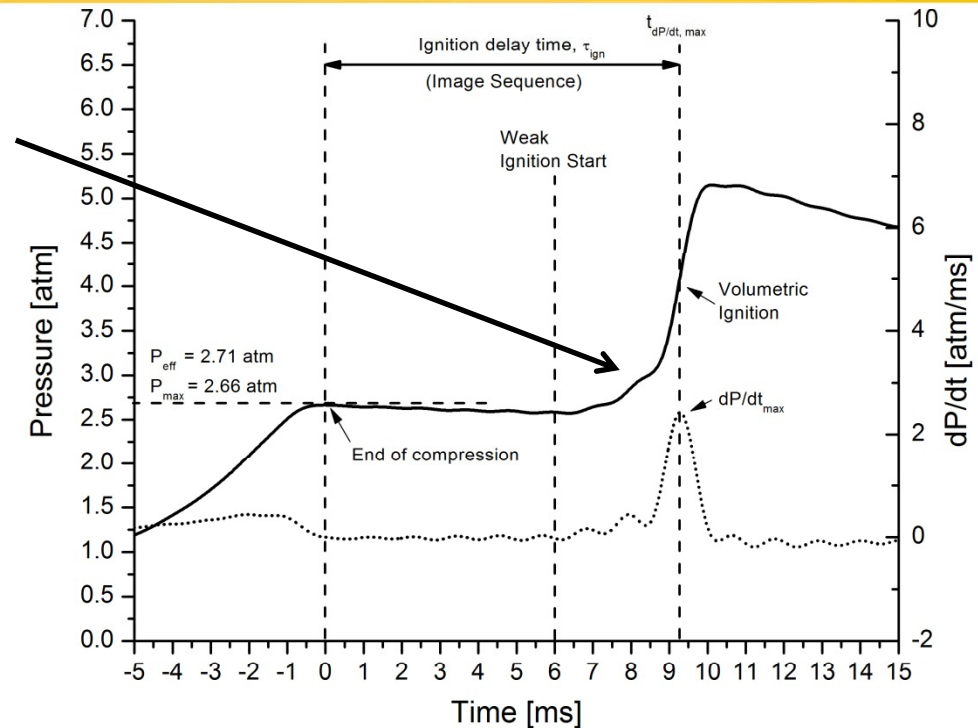
Digital imaging, high-speed color digital video camera: Vision Research, Phantom V7.11, Widescreen CMOS, 25,000 fps,  $512 \times 512$  pixels, exposure time of  $40 \mu\text{s}$



# Results: pressure time history of weak syngas ignition

Pressure time history reflects heat release from early localized ignition site.

- Pressure time history
- High-speed imaging
- $T = 1006 \text{ K}$ ,  $P = 2.71 \text{ atm}$
- Inert gas:  $\text{O}_2$  ratio = 5.91
- $\phi = 0.5$ ,
- 5.04%  $\text{H}_2$ , 7.26%  $\text{CO}$



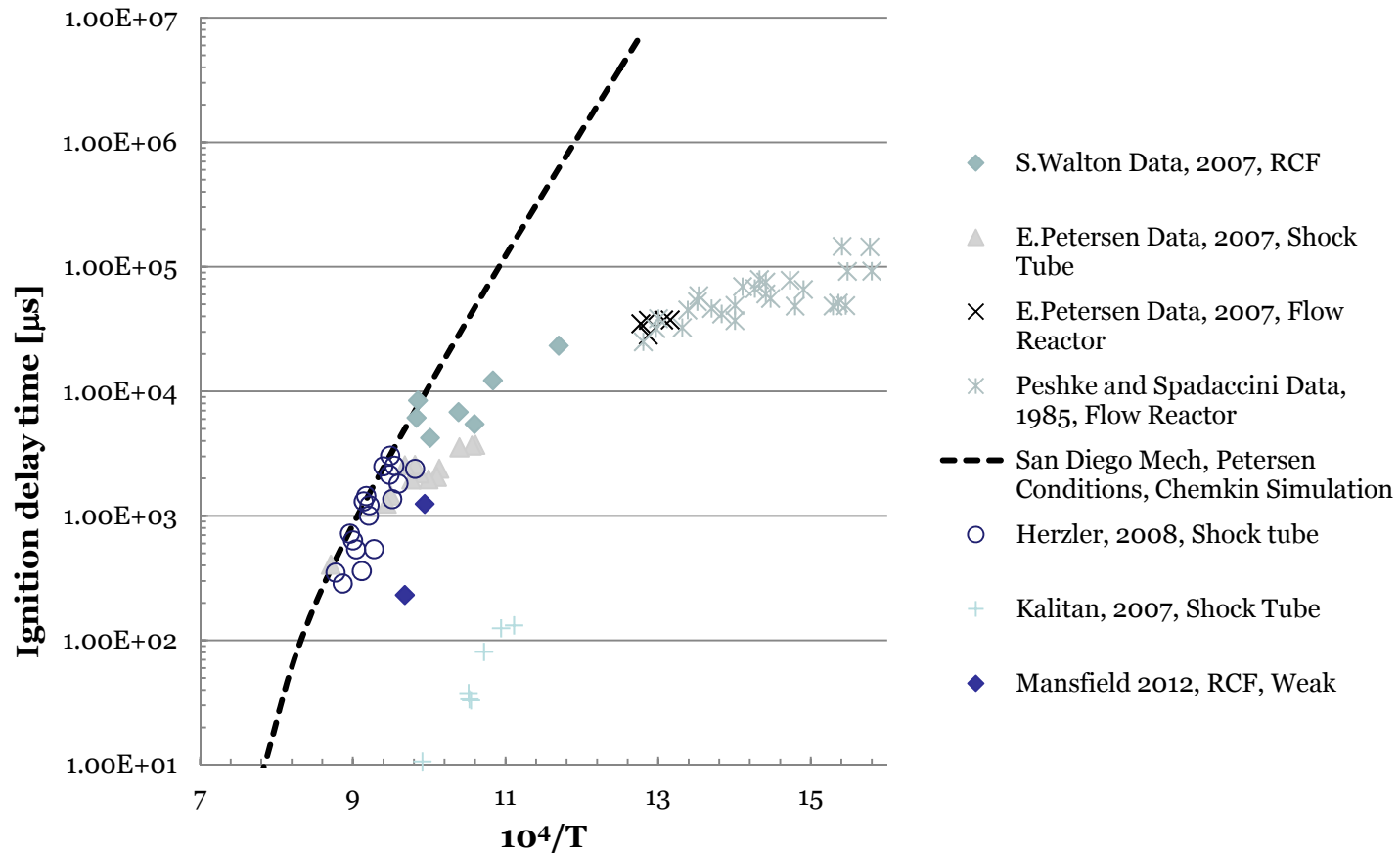
| $\phi$ | Test Gas Composition [%] <sup>a</sup> |             |              |              | $P_{eff}^b$<br>[atm] | $T_{eff}^b$<br>[K] | $\tau_{ig}^c$<br>[ms] | $\alpha(10^{-6})^d$<br>[m <sup>2</sup> /s] | $a^d$<br>[m/s] | Prop. Speed         |                | Predicted $\nabla T$ |                |
|--------|---------------------------------------|-------------|--------------|--------------|----------------------|--------------------|-----------------------|--|----------------|---------------------|----------------|----------------------|----------------|
|        | $\chi_{H_2}$                          | $\chi_{CO}$ | $\chi_{O_2}$ | $\chi_{N_2}$ |                      |                    |                       |  |                | $U_{prop}$<br>[m/s] | Error<br>[m/s] | Min.<br>[K/mm]       | Max.<br>[K/mm] |
| 0.15   | 3.6                                   | 2.4         | 19.8         | 74.3         | 7.1                  | 1011               | 15.8                  | 39.15                                      | 634.35         | S                   | -              | -                    | -              |
| 0.15   | 3.6                                   | 2.4         | 19.8         | 74.3         | 7.6                  | 1028               | 10.1                  | 37.54                                      | 639.35         | S                   | -              | -                    | -              |
| 0.15   | 3.6                                   | 2.4         | 19.8         | 74.3         | 14.9                 | 1033               | 9.6                   | 19.31                                      | 640.83         | S                   | -              | -                    | -              |
| 0.15   | 3.6                                   | 2.4         | 19.8         | 74.3         | 15.9                 | 1051               | 5.4                   | 18.58                                      | 646.07         | S                   | -              | -                    | -              |
| 0.15   | 3.6                                   | 2.4         | 19.8         | 74.3         | 8.1                  | 1046               | 4.9                   | 36.21                                      | 644.61         | S                   | -              | -                    | -              |
| 0.4    | 2.9                                   | 11.5        | 18           | 60           | 11.6                 | 1009               | 14                    | 21.59                                      | 614.66         | 2.76                | 0.05           | 3.22                 | 5.92           |
| 0.4    | 2.9                                   | 11.5        | 18           | 60           | 11.3                 | 1004               | 20.5                  | 21.99                                      | 613.22         | 2.41                | 0.05           | 2.47                 | 4.60           |
| 0.4    | 2.9                                   | 11.5        | 18           | 60           | 11.3                 | 1005               | 13.1                  | 22.03                                      | 613.51         | 2.68                | 0.01           | 3.55                 | 6.35           |
| 0.4    | 11.5                                  | 2.9         | 18           | 62.9         | 10.7                 | 994                | 7.7                   | 30.70                                      | 636.61         | 13.20               | 0.35           | 1.17                 | 2.20           |
| 0.4    | 2.9                                   | 11.5        | 18           | 63.5         | 11.4                 | 1009               | 11.1                  | 22.61                                      | 622.83         | 3.26                | 0.02           | 3.47                 | 6.23           |
| 0.4    | 7.2                                   | 7.2         | 18           | 63.2         | 23.5                 | 1015               | 7.2                   | 13.42                                      | 636.79         | 5.46                | 0.02           | 3.24                 | 5.80           |
| 0.4    | 7.2                                   | 7.2         | 18           | 63.2         | 11.0                 | 999                | 7.7                   | 25.60                                      | 625.43         | 8.02                | 0.29           | 1.94                 | 3.70           |
| 0.7    | 13.6                                  | 9.1         | 16.2         | 44.1         | 15.5                 | 923                | 15.8                  | 18.90                                      | 595.03         | 10.14               | 0.42           | 0.63                 | 1.22           |
| 1      | 24                                    | 16          | 20           | 17.6         | 14.1                 | 881                | 8.9                   | 25.72                                      | 600.44         | 32.16               | 0.49           | 0.33                 | 0.61           |
| 0.50   | 14.9                                  | 21.5        | 36.2         | 27.3         | 3.22                 | 1033               | 1.44                  | 144.5                                      | 667.45         | 63.07               | 4.08           | 2.07                 | 0.70           |
| 0.50   | 5.04                                  | 7.26        | 12.7         | 75           | 2.71                 | 1006               | 9.21                  | 117.3                                      | 639.25         | 7.30                | 1.09           | 2.77                 | 1.14           |
| 0.10   | 1.72                                  | 2.45        | 20.8         | 75           | -                    | -                  | -                     | -  | -              | S                   | -              | -                    | -              |

Note.

Red indicates 2012 work. The mixture composition is provided on a mole basis. The equivalence ratio is based on H<sub>2</sub> and CO to O<sub>2</sub> molar ratio. Experiments with strong or homogeneous ignition only are denoted "S".

<sup>a</sup> Balance CO<sub>2</sub>, <sup>b</sup> P<sub>eff</sub> and T<sub>eff</sub> defined in [1], <sup>c</sup> Measured [1], <sup>d</sup> Thermal diffusivity ( $\alpha$ ) and speed of sound ( $a$ ) based on T<sub>eff</sub> and unreacted mixture composition

All data scaled to 20 atm ( $P^{-1}$ ),  $\phi \cong 0.5$ ,  $H_2:CO \sim 1:1$



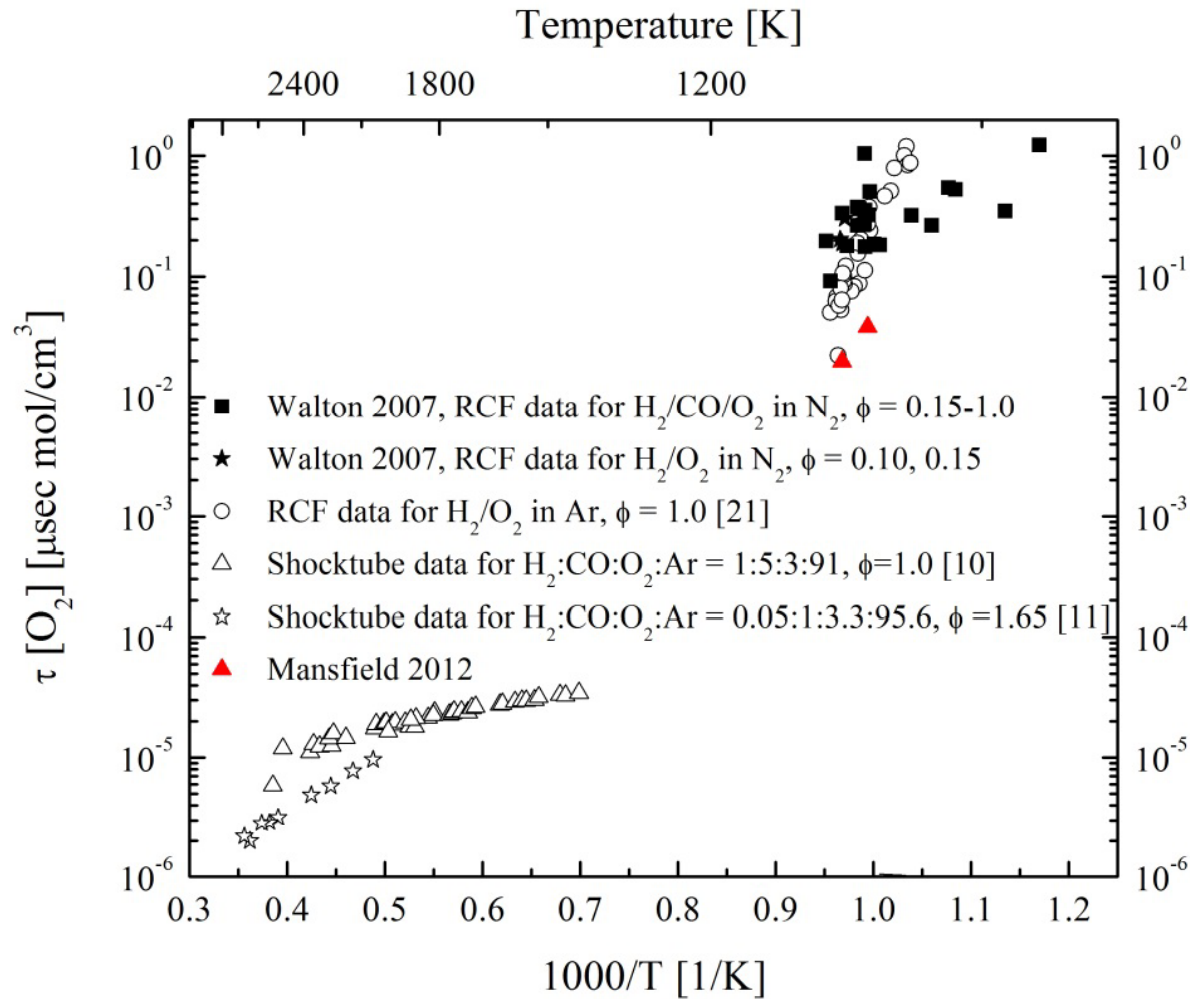
Kalitan, Mertens, Crofton, Petersen, (2007) *J. Prop. Power* 23 1291-1303

Petersen, Kalitan, Barrett, Reehal, Mertens, Beerer, Hack, McDonnell. (2007) *Comb. Flame* 149 244-247

Peschke, Spadaccini, (1985) Report No. EPRI AP-4291, Electric Power Research Institute

Herzler, Naumann (2008), *Comb. Sci. Tech.* 180 2015-2028

Walton, He, Zigler, Wooldridge, (2007) *Proc. Combust. Inst.* 31 3147-3154



Shock tube and RCF ignition data are highly complementary.

But ignition delay times only tell part of the story...

we can learn much more from ignition imaging.



## Goals of revisiting syngas high speed imaging data (1/2)

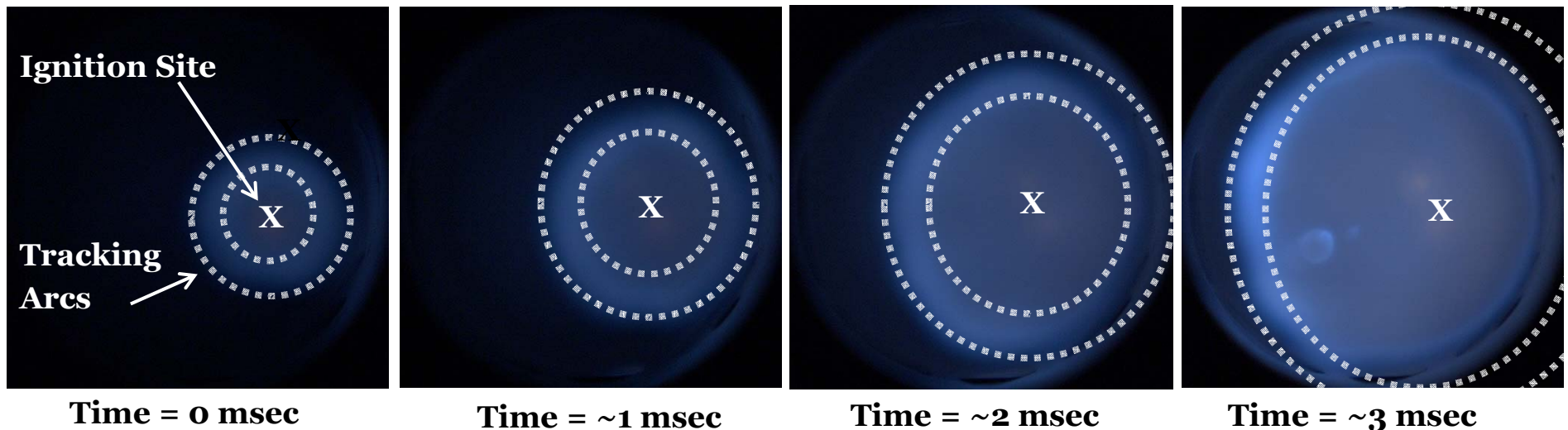
Apply iso-octane analysis<sup>2</sup> to previous and new syngas data<sup>1</sup> and evaluate existence of critical parameter(s) governing weak versus strong ignition behavior.

Quantify propagation speeds of reaction fronts.

Evaluate ignition theory and the implied thermal gradients

- Are the magnitudes feasible?
- What are possible causes?
- Consider hydrogen thermal properties

- Features were generally circular.
- Define arc center at initial site of local ignition
- Track reaction front radius as a function of time



- Identify maximum and minimum radius for each frame
- Apply linear regression
- Determine corresponding maximum and minimum speed

| $\phi$ | Test Gas Composition [%] <sup>a</sup> |             |              |              | $P_{eff}^b$<br>[atm] | $T_{eff}^b$<br>[K] | $\tau_{ig}^c$<br>[ms] | $\alpha(10^{-6})^d$<br>[m <sup>2</sup> /s] | $a^d$<br>[m/s] | Prop. Speed         |                | Predicted $\nabla T$ |                |
|--------|---------------------------------------|-------------|--------------|--------------|----------------------|--------------------|-----------------------|--|----------------|---------------------|----------------|----------------------|----------------|
|        | $\chi_{H_2}$                          | $\chi_{CO}$ | $\chi_{O_2}$ | $\chi_{N_2}$ |                      |                    |                       |  |                | $U_{prop}$<br>[m/s] | Error<br>[m/s] | Min.<br>[K/mm]       | Max.<br>[K/mm] |
| 0.15   | 3.6                                   | 2.4         | 19.8         | 74.3         | 7.1                  | 1011               | 15.8                  | 39.15                                      | 634.35         | S                   | -              | -                    | -              |
| 0.15   | 3.6                                   | 2.4         | 19.8         | 74.3         | 7.6                  | 1028               | 10.1                  | 37.54                                      | 639.35         | S                   | -              | -                    | -              |
| 0.15   | 3.6                                   | 2.4         | 19.8         | 74.3         | 14.9                 | 1033               | 9.6                   | 19.31                                      | 640.83         | S                   | -              | -                    | -              |
| 0.15   | 3.6                                   | 2.4         | 19.8         | 74.3         | 15.9                 | 1051               | 5.4                   | 18.58                                      | 646.07         | S                   | -              | -                    | -              |
| 0.15   | 3.6                                   | 2.4         | 19.8         | 74.3         | 8.1                  | 1046               | 4.9                   | 36.21                                      | 644.61         | S                   | -              | -                    | -              |
| 0.4    | 2.9                                   | 11.5        | 18           | 60           | 11.6                 | 1009               | 14                    | 21.59                                      | 614.66         | 2.76                | 0.05           | 3.22                 | 5.92           |
| 0.4    | 2.9                                   | 11.5        | 18           | 60           | 11.3                 | 1004               | 20.5                  | 21.99                                      | 613.22         | 2.41                | 0.05           | 2.47                 | 4.60           |
| 0.4    | 2.9                                   | 11.5        | 18           | 60           | 11.3                 | 1005               | 13.1                  | 22.03                                      | 613.51         | 2.68                | 0.01           | 3.55                 | 6.35           |
| 0.4    | 11.5                                  | 2.9         | 18           | 62.9         | 10.7                 | 994                | 7.7                   | 30.70                                      | 636.61         | 13.20               | 0.35           | 1.17                 | 2.20           |
| 0.4    | 2.9                                   | 11.5        | 18           | 63.5         | 11.4                 | 1009               | 11.1                  | 22.61                                      | 622.83         | 3.26                | 0.02           | 3.47                 | 6.23           |
| 0.4    | 7.2                                   | 7.2         | 18           | 63.2         | 23.5                 | 1015               | 7.2                   | 13.42                                      | 636.79         | 5.46                | 0.02           | 3.24                 | 5.80           |
| 0.4    | 7.2                                   | 7.2         | 18           | 63.2         | 11.0                 | 999                | 7.7                   | 25.60                                      | 625.43         | 8.02                | 0.29           | 1.94                 | 3.70           |
| 0.7    | 13.6                                  | 9.1         | 16.2         | 44.1         | 15.5                 | 923                | 15.8                  | 18.90                                      | 595.03         | 10.14               | 0.42           | 0.63                 | 1.22           |
| 1      | 24                                    | 16          | 20           | 17.6         | 14.1                 | 881                | 8.9                   | 25.72                                      | 600.44         | 32.16               | 0.49           | 0.33                 | 0.61           |
| 0.50   | 14.9                                  | 21.5        | 36.2         | 27.3         | 3.22                 | 1033               | 1.44                  | 144.5                                      | 667.45         | 63.07               | 4.08           | 2.07                 | 0.70           |
| 0.50   | 5.04                                  | 7.26        | 12.7         | 75           | 2.71                 | 1006               | 9.21                  | 117.3                                      | 639.25         | 7.30                | 1.09           | 2.77                 | 1.14           |
| 0.10   | 1.72                                  | 2.45        | 20.8         | 75           | -                    | -                  | -                     | -  | -              | S                   | -              | -                    | -              |

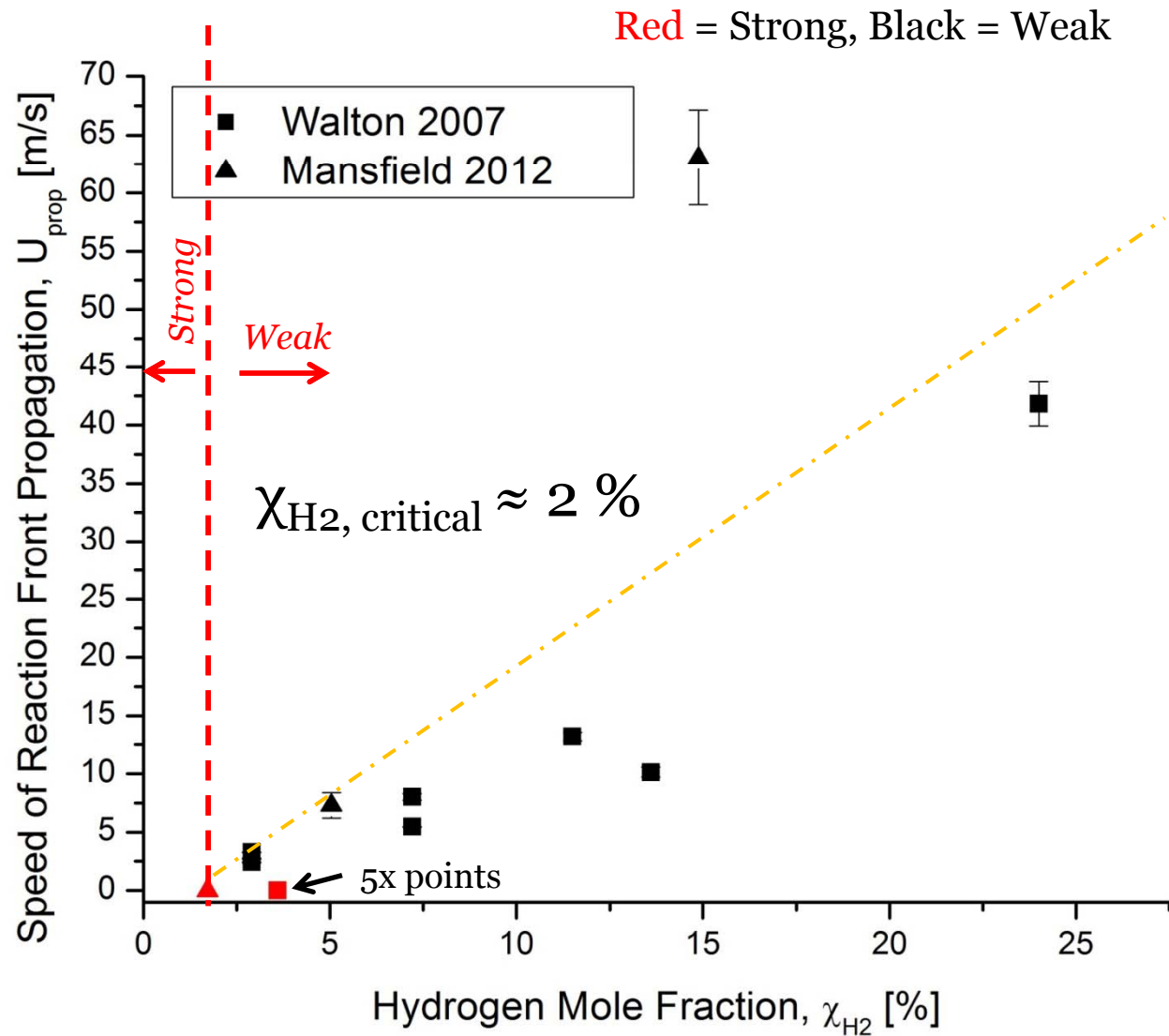
Note.

Red indicates 2012 work. The mixture composition is provided on a mole basis. The equivalence ratio is based on H<sub>2</sub> and CO to O<sub>2</sub> molar ratio. Experiments with strong or homogeneous ignition only are denoted "S".

<sup>a</sup> Balance CO<sub>2</sub>, <sup>b</sup> P<sub>eff</sub> and T<sub>eff</sub> defined in [1], <sup>c</sup> Measured [1], <sup>d</sup> Thermal diffusivity ( $\alpha$ ) and speed of sound ( $a$ ) based on T<sub>eff</sub> and unreacted mixture composition



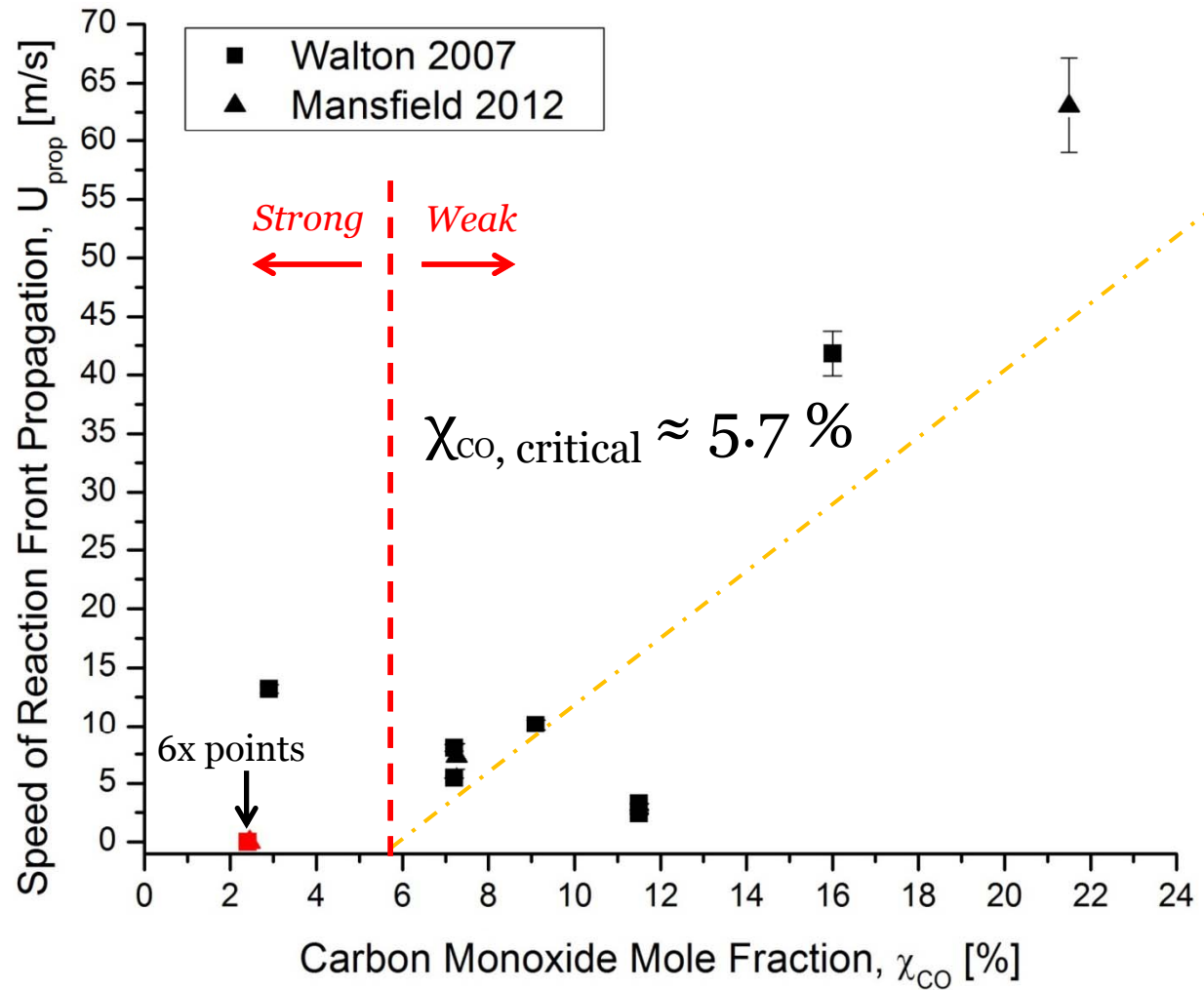
- What factors dominate ignition response,  $\chi_{H_2}$ ,  $\chi_{CO}$ , etc.?
- Critical mole fraction is defined as intercept
- Propagation rates increase with increase  $H_2$  mole fraction
- Critical  $H_2$  mole fraction is consistent with experimental observations...



# Results: Propagation speed as a $\chi_{CO}$

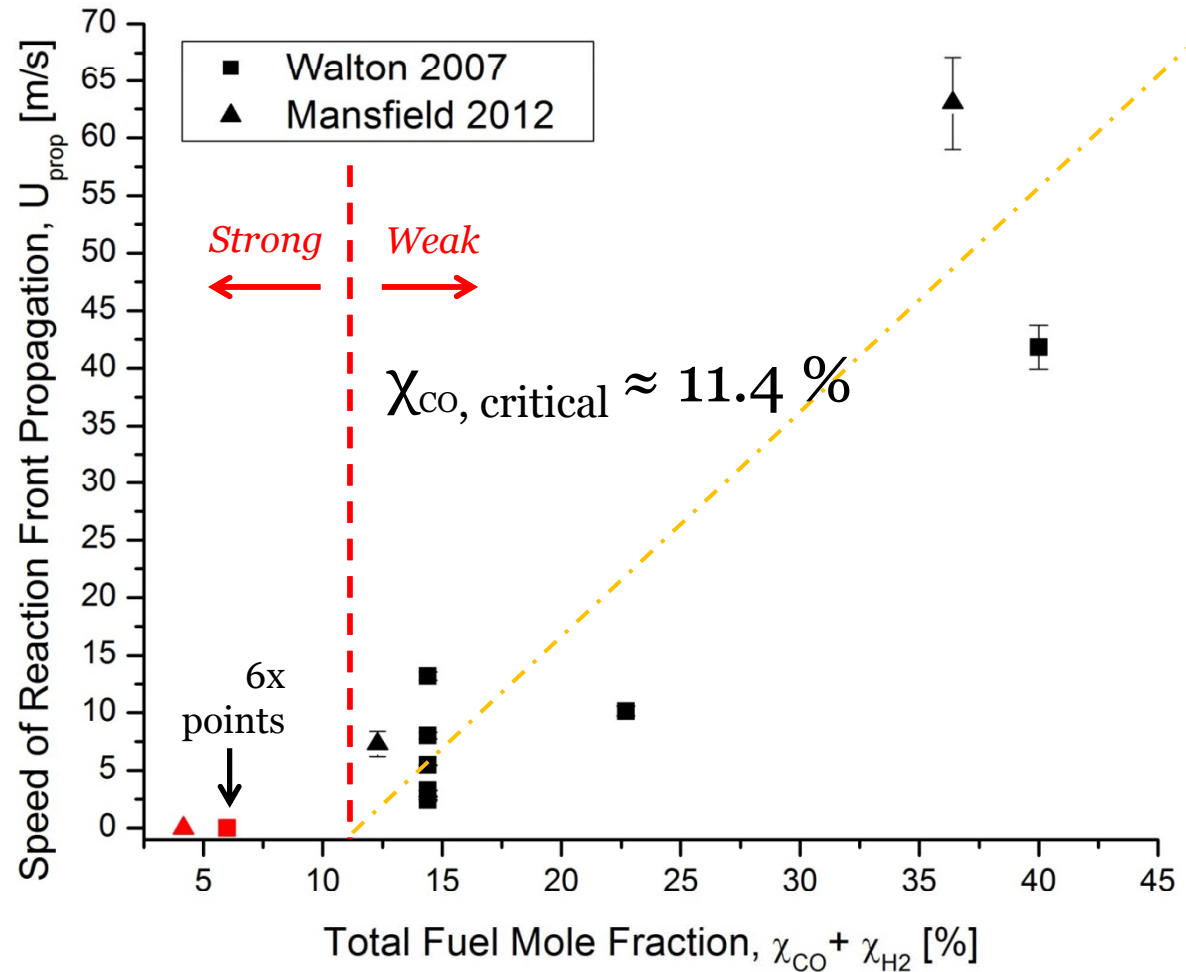
Red = Strong, Black = Weak

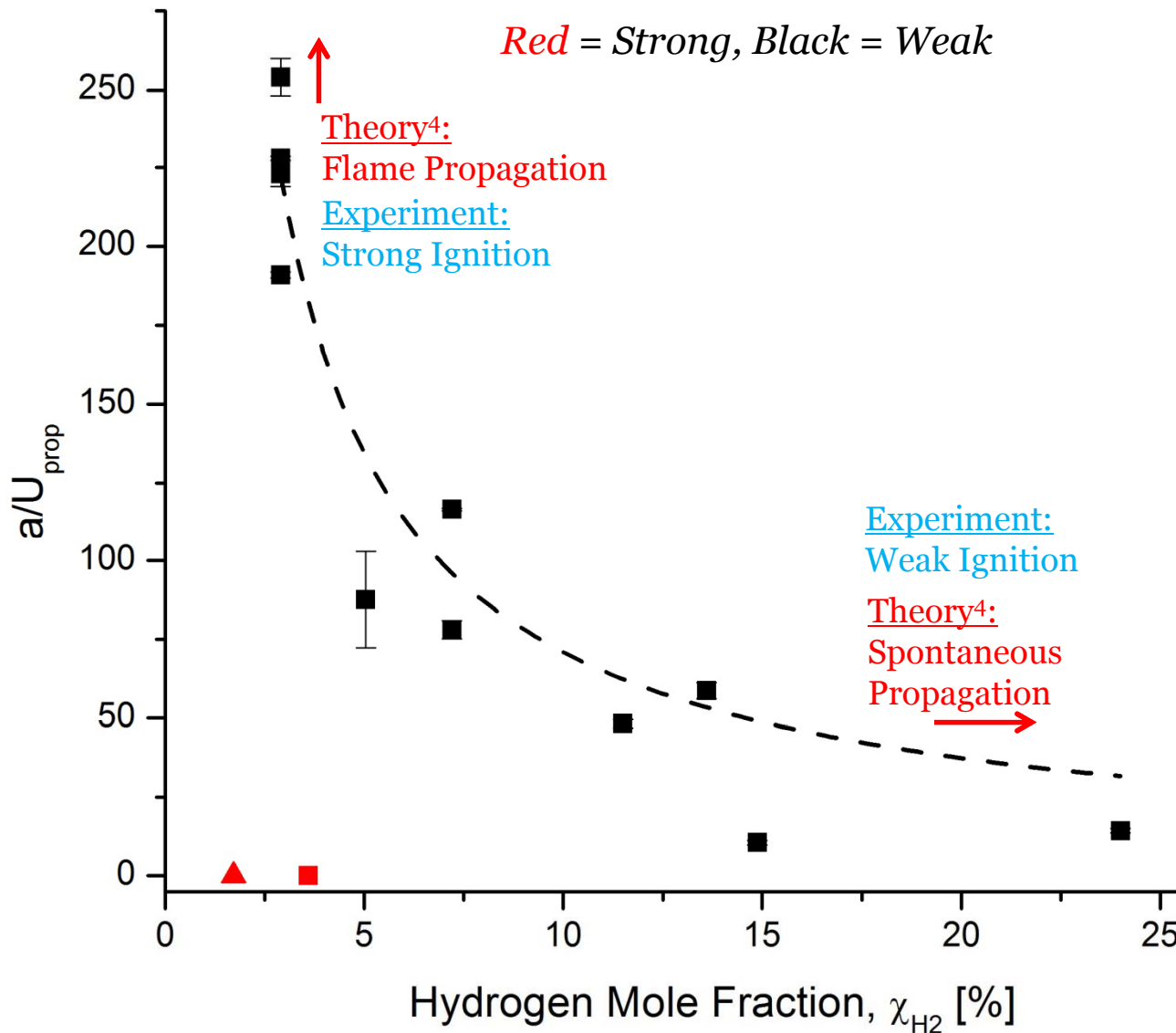
CO criteria appears comparable in quality of fit to data and trends for ignition regimes as  $H_2$  criteria...



Total fuel is an equally good measure of propagation rate and ignition regime criteria.

Red = Strong, Black = Weak





## Weak Ignition

- Autoignition is slow and reaction fronts are sufficiently fast to affect induction period

## Strong Ignition

- Autoignition is fast and reaction fronts are too slow to affect induction period

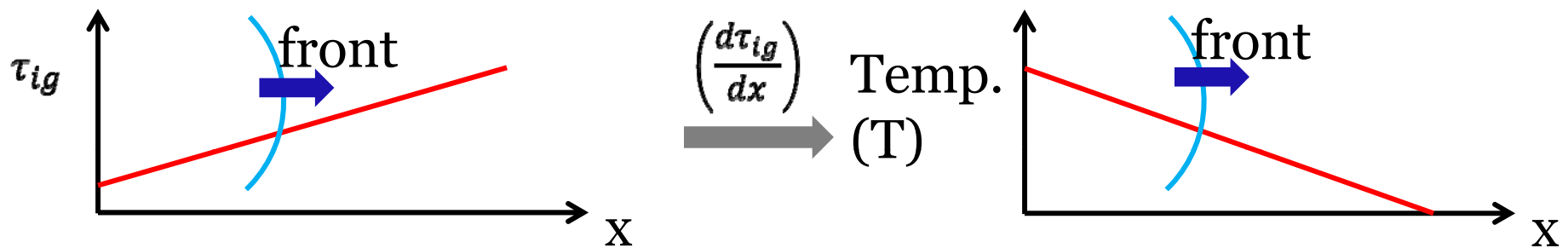
## Balance of time scales

- Strong:  $\tau_{ignition}$
- Weak:  $\frac{L}{U_{prop}}$

\*a = speed of sound, L = characteristic length in reaction chamber (diameter)

- Zeldovich Ignition Theory<sup>5</sup>:

- Propagation Speeds ( $U_{prop}$ )  $\gg$  Laminar Flame Speed, so  $U_{prop} = |\nabla\tau_{ig}|^{-1}$



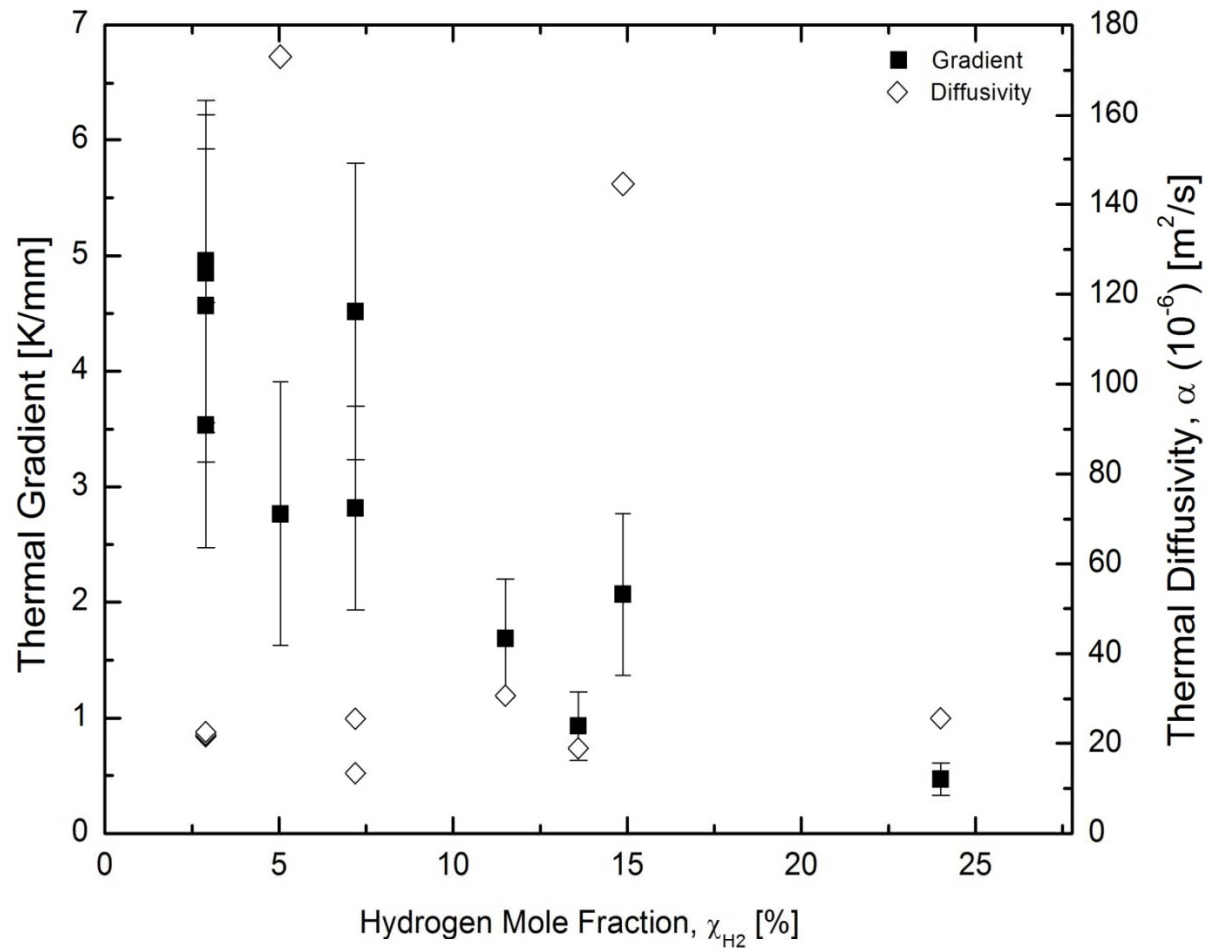
- Assume  $\nabla\tau_{ig} = \frac{\partial\tau_{ig}}{\partial T} \nabla T$  then,  $\nabla T = \left( \left( \frac{\partial\tau_{ig}}{\partial T} \right) U_{prop} \right)^{-1}$

- Walton et al<sup>1</sup>:  $\tau_{ig} = 3.7(10^{-6})P^{-0.5}\phi^{-0.4}\chi_{O_2}^{-5.4} \exp\left(\frac{12,500}{RT}\right)$ , so

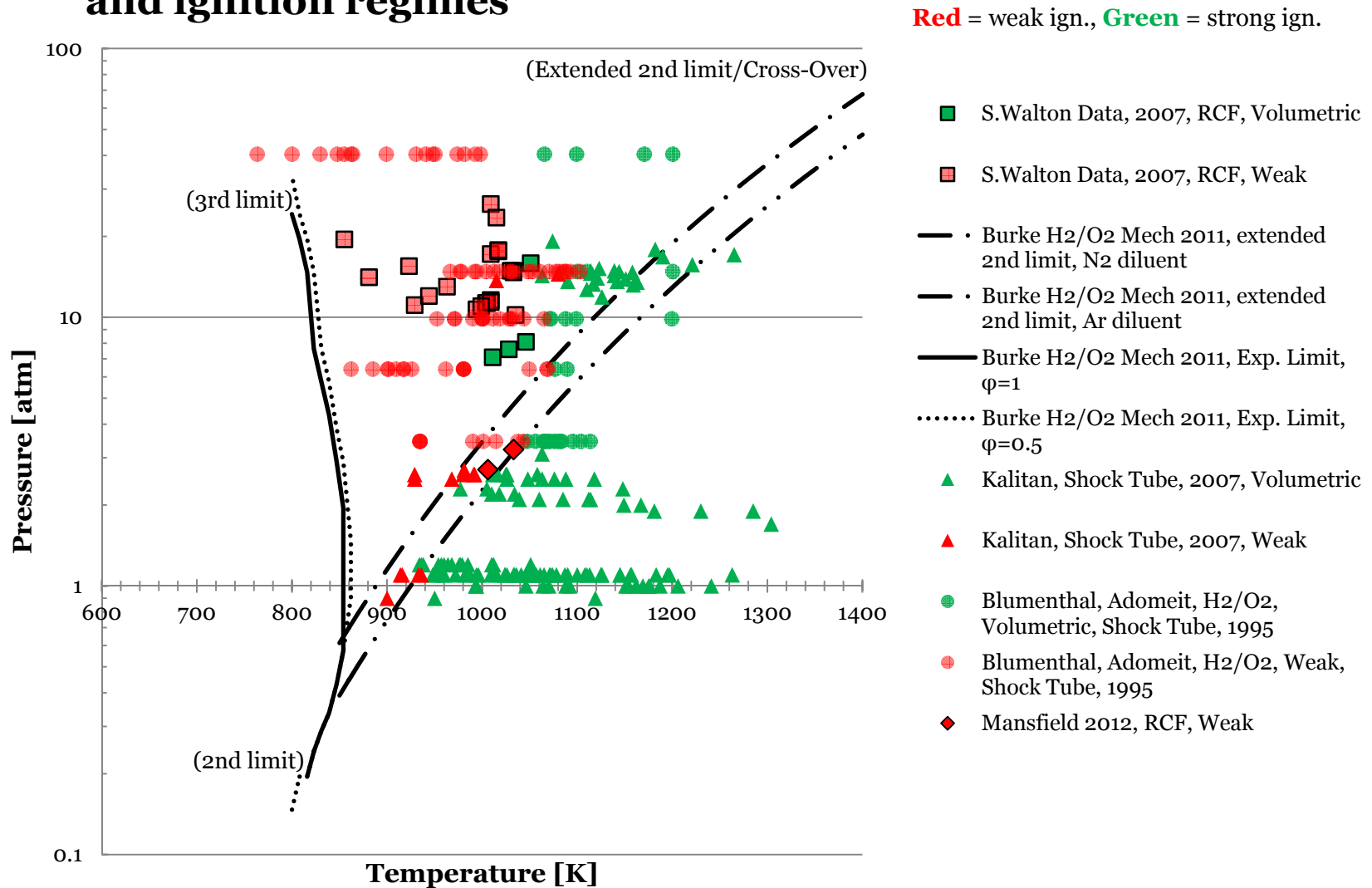
$$\frac{\partial\tau_{ig}}{\partial T} = \tau_{ig} * \frac{12,500}{RT^2}$$

$$\nabla T = \nabla T(\tau_{ig}, T, U_{prop})$$

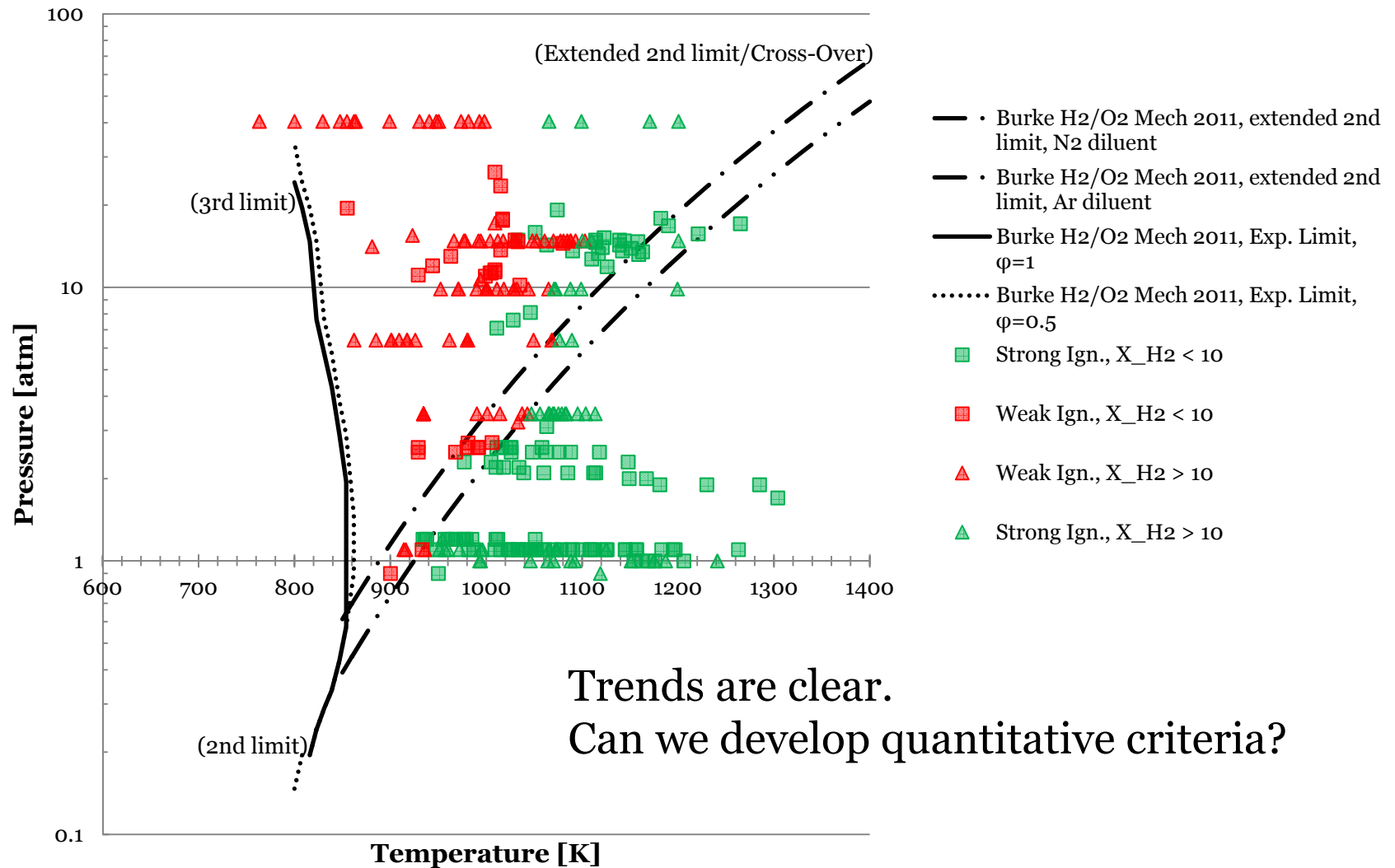
- Calculated thermal gradients required to produce observed speeds are realistic; consistent with expectations based on previous UM RCF and other measurements (Donovan et al.<sup>6</sup>, Strozzi et al.<sup>7</sup>)
- No apparent dependence on thermal diffusivity.



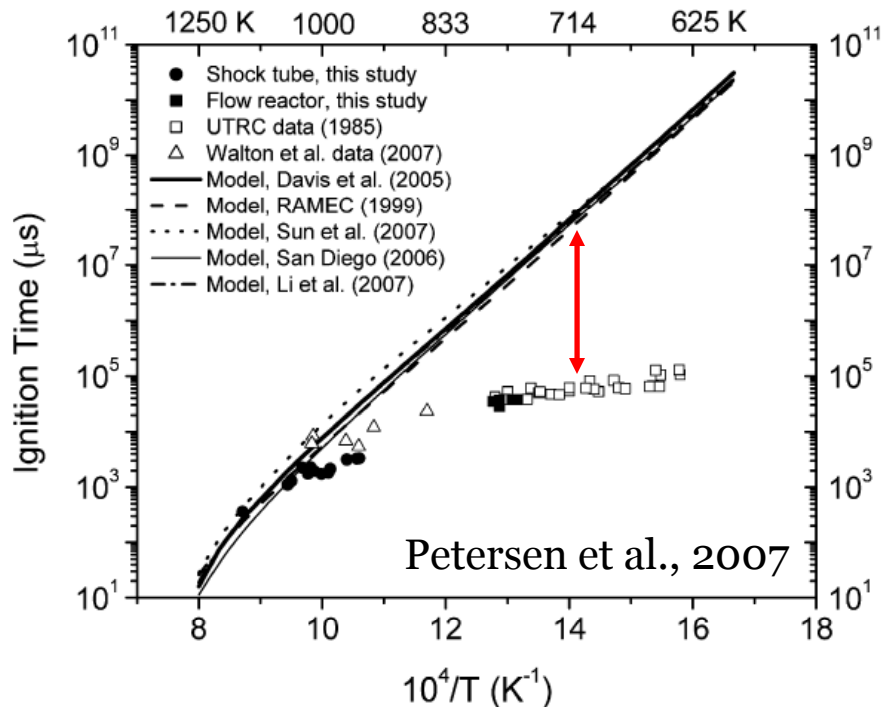
**There is a strong correlation between explosion limits and ignition regimes**



## H<sub>2</sub> concentration may shift regime boundary







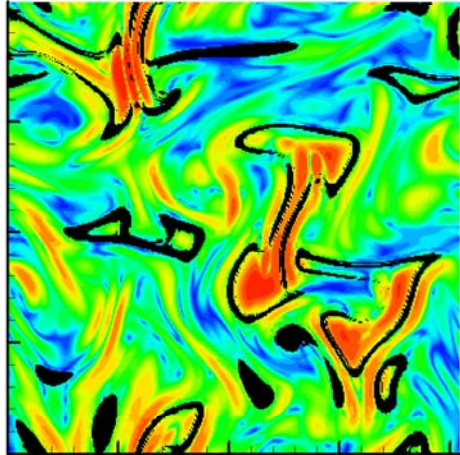
**Discrepancy** in ignition delay between the experiments and numerical modeling approaches has not been understood properly

Possible explanations:

- Uncertainties in rate coefficients
- Incomplete reaction mechanisms
- Surface-catalytic mechanisms
- Ignition regimes
- Wall heat transfer
- Turbulence (Ihme, C&F, 2012)

- Enhances auto-ignition by facilitating heat and radical transfer into the cold regions (**Ignition kernel**)
- Delays auto-ignition by removing the heat and radicals from the hot regions (**Homogeneous ignition**)

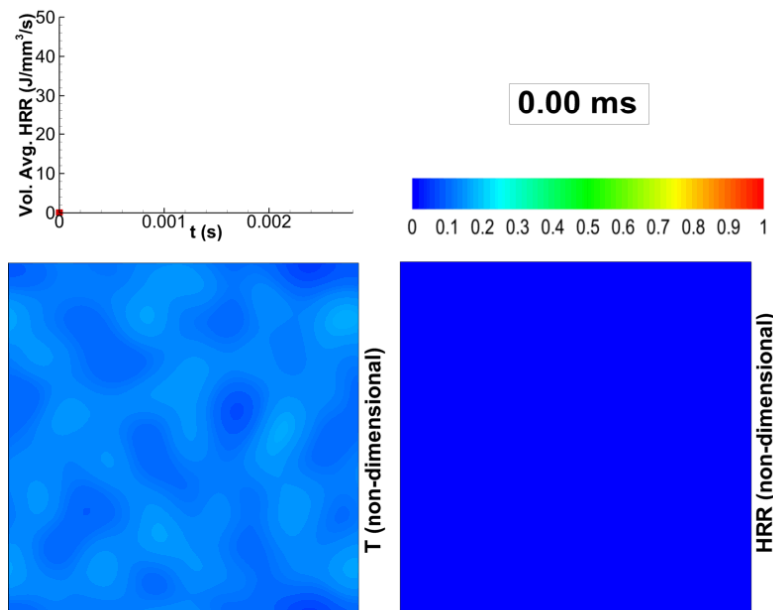
**Under which parametric conditions of temperature and turbulence intensity are the above effects dominant for syngas mixtures?**



H<sub>2</sub>/air auto-ignition

Ignition of H<sub>2</sub>/Air Mixture with Temperature and Composition Stratification (Bansal & Im, C&F, 2011; Gupta, Im, Valorani, Proc. Comb. Inst., 2011)

- Positively- vs. negatively-correlated T- $\phi$  fluctuations
- Overall effects on ignition delay and burn duration
- Computational singular perturbation (CSP) for automated identification of ignition regimes (homogeneous ignition, spontaneous front propagation, deflagration)



n-heptane/air 2-stage auto-ignition

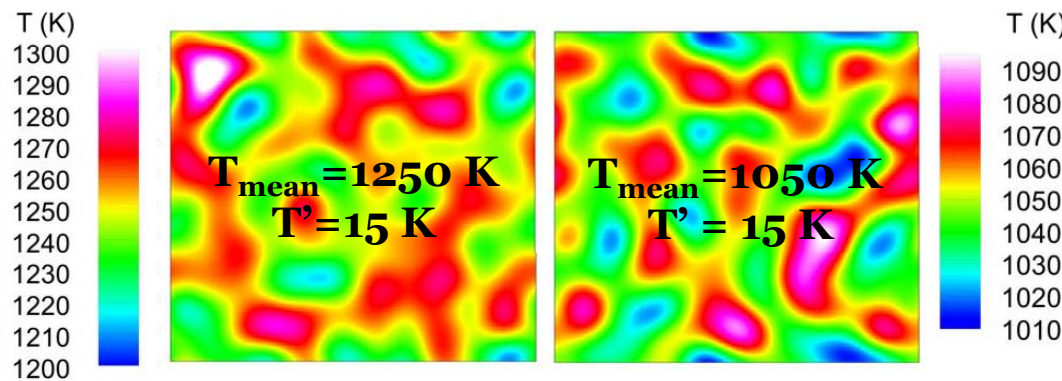
Ignition of n-Heptane/Air Mixture with Temperature and Composition Stratification (Gupta, Im, Valorani, Proc. Comb. Inst., 2013)

- CSP used to analyze ignition regimes during the 1<sup>st</sup> and 2<sup>nd</sup> stage ignition events
- 2-stage ignition (NTC chemistry) promotes the overall ignition characteristics in spontaneous ignition regime

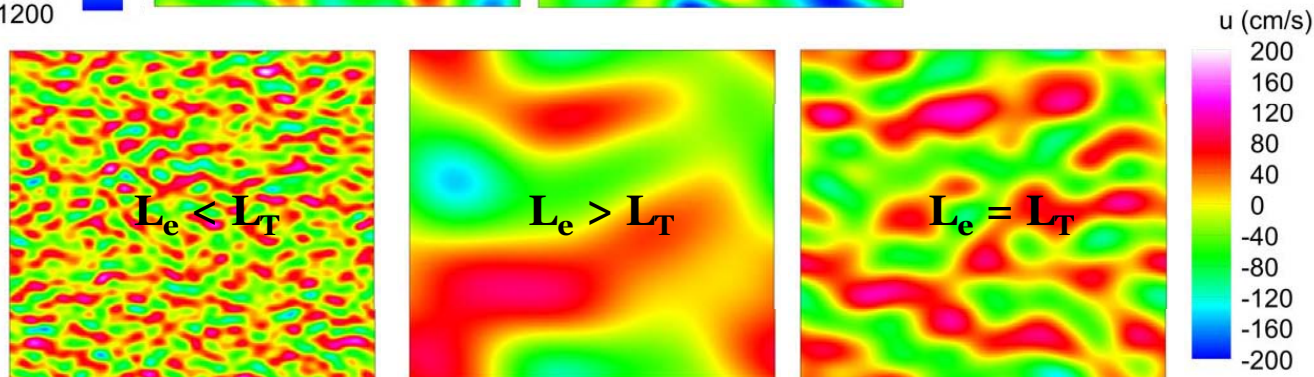
**What was NOT considered:**

- Effects of turbulence-chemistry interaction on autoignition when the length and time scales for temperature and flow fields are different.

- Syngas chemical mechanism: (Li et al., 2007)
- 2D square domain with periodic boundary conditions (compression heating accounted for)
- Prescribed initial turbulence and temperature spectrum at different length scales
- Initial pressure at 20 atm and uniform mixture:  $\phi = 0.5$  (Petersen et al., 2007)
- Initial temperatures: 1050 K (Low Temperature Chemistry), 1250 K (High Temperature Chemistry)



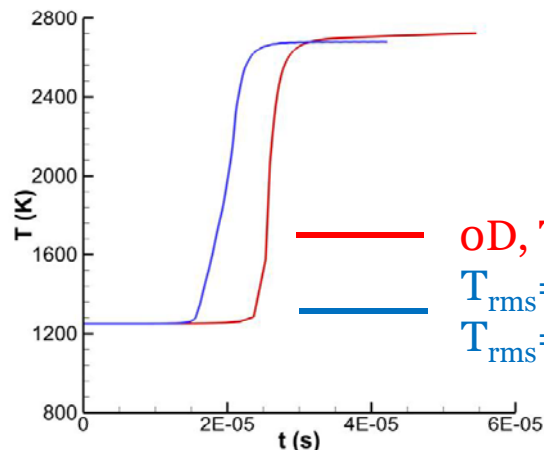
Explore the effect of high vs. low temperature chemistry



Explore the effect of small vs. large scale turbulent mixing

## 1D Domain with Periodic Boundaries, 20 atm, $\phi = 0.5$

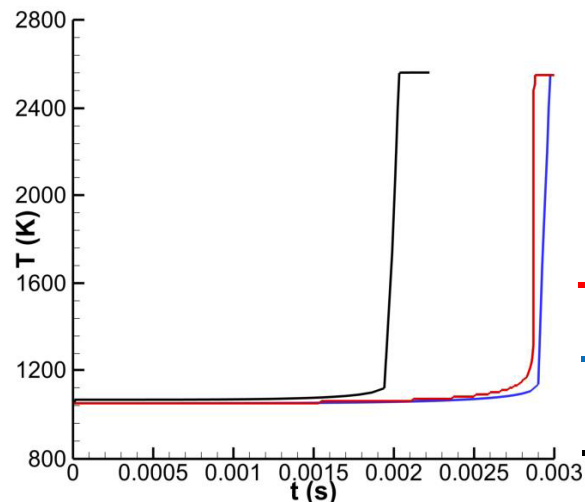
- Sinusoidal temperature field:  $T = T_{\text{mean}} \sin(2\pi X/L)$
- Sinusoidal velocity field:  $u = u_{\text{mean}} \sin(2\pi X/\lambda_u)$



$$T_{\text{mean}} = 1250 \text{ K}$$

- Temperature stratifications **reduce** the ignition delay
- Velocity perturbations have little effect

—  $oD, T = T_{\text{mean}}$   
 —  $T_{\text{rms}} = 10 \text{ K}, u_{\text{rms}} = 0 \text{ cm/s}$   
 —  $T_{\text{rms}} = 10 \text{ K}, u_{\text{rms}} = 50 \text{ cm/s}, \lambda_u = 0.1L$

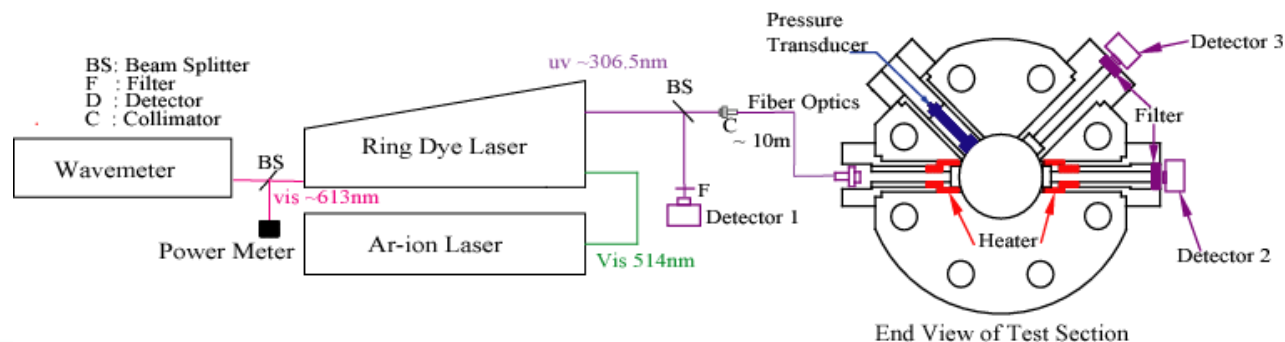


$$T_{\text{mean}} = 1050 \text{ K}$$

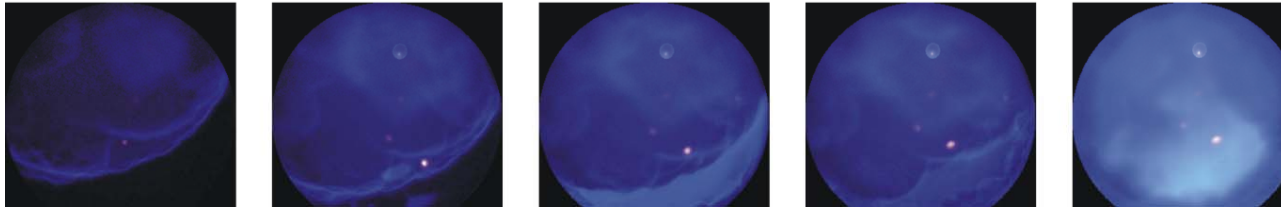
- Temperature stratifications **marginally increase** the ignition delay (*needs further investigation*)
- Very large velocity perturbations significantly decrease the ignition delay (*needs further investigation*)

—  $oD, T = T_{\text{mean}}$   
 —  $T_{\text{rms}} = 10 \text{ K}, u_{\text{rms}} = 0 \text{ cm/s}$   
 —  $T_{\text{rms}} = 10 \text{ K}, u_{\text{rms}} = 50 \text{ cm/s}, \lambda_u = 0.1L$   
 —  $T_{\text{rms}} = 10 \text{ K}, u_{\text{rms}} = 5000 \text{ cm/s}, \lambda_u = 0.1L$

- Source of local ignition remains unknown, but the signature phenomena (early pressure rise) are observed in multiple facilities, and links to state and composition conditions are becoming more clear.
- Additional UM RCF and UM Computational Experiments:
  - Systematic exploration of thermal, gas dynamic and composition effects on syngas ignition, particulate disturbances, H<sub>2</sub> mass diffusion effects, and OH measurements.
  - Develop unifying theory to describe conditions likely to be affected by transport/chemistry interactions
  - Isolate and possibly identify sources of local ignition



thank you



The authors acknowledge the generous financial support of the Department of Energy, National Energy Technology Laboratory via the University Turbine Systems Research Program and the University of Michigan.



- [1] S. M. Walton, X. He, B. T. Zigler, and M. S. Wooldridge, "An experimental investigation of the ignition properties of hydrogen and carbon monoxide mixtures for syngas turbine applications," *Proceedings of the Combustion Institute*, vol. 31, no. 2, pp. 3147-3154, Jan. 2007.
- [2] S. Walton, X. He, B. Zigler, M. Wooldridge, and a Atreya, "An experimental investigation of iso-octane ignition phenomena," *Combustion and Flame*, vol. 150, no. 3, pp. 246-262, Aug. 2007.
- [3] M. Chaos and F. L. Dryer, "Syngas Combustion Kinetics and Applications," *Combustion Science and Technology*, vol. 180, no. 6, pp. 1053-1096, May 2008.
- [4] Y. Zeldovich, "Regime classification of an exothermic reaction with nonuniform initial conditions," *Combustion and Flame*, vol. 39, no. 2, pp. 211-214, Oct. 1980.
- [5] X. J. Gu, D. R. Emerson, and D. Bradley, "Modes of reaction front propagation from hot spots," *Combustion and Flame*, vol. 133, no. 1-2, pp. 63-74, Apr. 2003.
- [6] M. T. Donovan, X. He, B. T. Zigler, T. R. Palmer, M. S. Wooldridge, and a. Atreya, "Demonstration of a free-piston rapid compression facility for the study of high temperature combustion phenomena," *Combustion and Flame*, vol. 137, no. 3, pp. 351-365, May 2004.
- [7] C. Strozzi, J. Sotton, A. Mura, and M. Bellenoue, "Characterization of a two-dimensional temperature field within a rapid compression machine using a toluene planar laser-induced fluorescence imaging technique," *Measurement Science and Technology*, vol. 20, no. 12, p. 125403, Dec. 2009.
- [8] M. Kaviany, *Principles of Heat Transfer*. John Wiley & Sons, Inc., 2002, p. 279.
- [9] R. Blumenthal, K. Fieweger, and K. Komp, "Gas dynamic features of self ignition of non diluted fuel/air mixtures at high pressure," *science and technology*, no. 2012, pp. 37-41, 1996.
- Kalitan, D.M., Mertens, J.D., Crofton, M.W., Petersen, E.L. (2007) *J. Prop. Power* 23 1291-1303